















S/C/L-Band Transmission in Few-Mode MCF with Optical Frequency Comb Regeneration via Single-Mode Core Seed Distribution

Daniele Orsuti , Benjamin J. Puttnam , *Member, IEEE*, Ruben S. Luís , *Senior Member, IEEE*, Manuel S. Neves , Menno van den Hout , Giammarco Di Sciullo , Divya A. Shaji, Budsara Boriboon , Georg Rademacher , *Senior Member, IEEE*, Jun Sakaguchi , *Member, IEEE*, Cristian Antonelli , *Senior Member, IEEE*, Chigo Okonkwo , *Senior Member, IEEE*, Paulo P. Monteiro , Fernando P. Guiomar , Luca Palmieri , *Senior Member, IEEE*, and Hideaki Furukawa, *Member, IEEE*

Abstract—We demonstrate parametric optical frequency comb (OFC) regeneration based on a transmitted seed in a high spatial density SDM fiber with 114 spatial channels and a seed distribution core. We show that such a fiber is compatible with ultra-high data rate links in a recently proposed network architecture that exploits the synergy between SDM fibers and OFC technology, extending this network concept to include few-mode cores for the first time. The employed OFCs support the generation of 650 x 25 GHz-spaced carriers covering the S/C/L-band for a total useful bandwidth of 134 nm, i.e., 50% wider than previously demonstrated with an OFC. Data rates of approximately 330 Tb/s per few-mode core are measured, with a potential of more than 12.7 Pb/s per fiber. We show that the use of OFCs for both transmission and detection simplifies coherent reception with a 3 orders of magnitude lower frequency offset compared to conventional intradyne schemes. We also show that

the phase coherence among the comb carriers can be exploited to share digital signal processing (DSP) resources among the received channels. These results demonstrate the potential of OFCs for high-capacity networking, capable of replacing hundreds of transceiver lasers in each node and simplifying the DSP through the use of coherent and frequency-locked carriers.

Index Terms—Parametric optical frequency comb, comb regeneration, space-division multiplexing, seeded multi-core fiber network, frequency locked detection, intradyne detection.

I. INTRODUCTION

THE increasing demand for high-throughput data services has driven research into networks that combine both wavelength-division multiplexing (WDM) and space-division multiplexing (SDM). In this context, parametric optical frequency combs (OFCs) have the unique capability of providing hundreds of high-quality carriers across bandwidths spanning tens of nanometers, with the potential of replacing hundreds of transceiver lasers [1], [2]. Additionally, the extreme stability, equidistant spacing, and phase coherence of the comb carriers can be exploited to minimize the spectral guard band between WDM channels [3], and implement shared digital signal processing (DSP) schemes [4]. For these reasons, OFCs are a promising solution for cost-sensitive applications, such as intra- and inter-datacenter networks where there is the need to simultaneously meet the requirements of high capacity, simple transceiver architecture, and reduced DSP complexity.

Manuscript received XX June XXXX; revised XX August XXX and XXX September 2023; revised XX September XXX.

This work was supported in part by the Italian Ministry for Education, University and Research (MIUR), “Departments of Excellence” under Grant law 232/2016, in part by the Project Fiber Infrastructure for Research on Space-division multiplexed Transmission (FIRST) under Grant PRIN 2017 (Corresponding author: *Daniele Orsuti*.)

Daniele Orsuti is with the Photonic Network Laboratory, National Institute of Information and Communications Technology, Tokyo 184-8795, Japan, and also with the Department of Information Engineering, University of Padova, 35131 Padova, Italy (e-mail: daniele.orsuti@phd.unipd.it).

Benjamin J. Puttnam, Ruben S. Luís, Budsara Boriboon, Jun Sakaguchi, and Hideaki Furukawa are with the Photonic Network Laboratory, National Institute of Information and Communications Technology, Tokyo 184-8795, Japan (e-mail: ben@nict.go.jp; rluis@nict.go.jp; budsara@nict.go.jp; jsakaguchi@nict.go.jp; furukawa@nict.go.jp).

Manuel S. Neves, Paulo P. Monteiro, and Fernando P. Guiomar are with the Instituto de Telecomunicações, University of Aveiro, 3810-193 Aveiro, Portugal (e-mail: msneves@ua.pt; paulo.monteiro@ua.pt; guiomar@av.it.pt).

Menno van den Hout and Chigo Okonkwo, are with the High Capacity Optical Transmission Laboratory, Electro-Optical Communications Group, Eindhoven University of Technology, 5600 MB Eindhoven, The Netherlands (e-mail: m.v.d.hout@tue.nl; c.m.okonkwo@tue.nl).

Georg Rademacher was with the Photonic Network Laboratory, National Institute of Information and Communications Technology, Koganei 184-8795, Japan. He is now with the Institute of Electrical and Optical Communications, University of Stuttgart, 70174 Stuttgart, Germany (e-mail: georg.rademacher@int.uni-stuttgart.de).

Giammarco Di Sciullo, Divya A. Shaji, and Cristian Antonelli are with the University of L’Aquila and CNIT, 67100 L’Aquila, Italy (e-mail: giammarco.disciullo@graduate.univaq.it; divyaann.shaji, cristian.antonelli@univaq.it).

Luca Palmieri is with the Department of Information Engineering, University of Padova, 35131 Padova, Italy (e-mail: luca.palmieri@unipd.it).

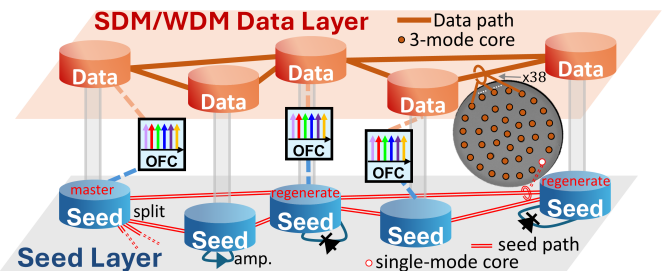


Fig. 1. Diagram of comb-based SDM/WDM network supported by seed transmission layer to allow comb regeneration in MCF connected nodes.

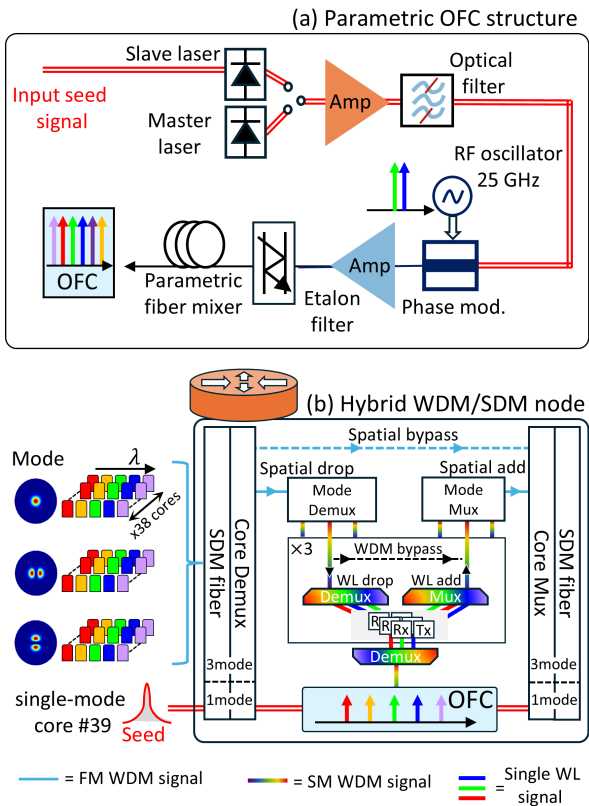


Fig. 2. (a) Structure of the parametric OFC, and (b) Comb-based network node allowing hybrid SDM-WDM add-drop multiplexing. FM: few-mode; SM: single-mode; WL: wavelength.

Another interesting feature of OFCs is the possibility to remotely regenerate a synchronized comb using a broadcast seed signal [5]–[8]. The regenerated combs can act as synchronized local-oscillators (LOs) allowing coherent detection with frequency-locked transceiver carriers. Previous studies have reported comb regeneration over moderate bandwidths of less than 11 nm per transmitted seed [5]–[8]. More recently, a novel parametric comb structure has enabled the transmission and regeneration of 80-nm-wide combs spanning the C and L-bands [9], [10], introducing the MCF-seeded comb optical network (MCF-SCON) architecture [10], which utilizes the synergy between OFCs and SDM fibers to support low-complexity high-capacity data networks.

Here, we extend our previous publication [11], where we propose to include in this network concept also few-mode MCFs (FM-MCFs) for ultra-high capacity links using a dedicated novel SDM fiber. The fiber has 38×3 few-mode cores for data transmission, and a 39th single-mode core for transmission of the comb seed signal; a cross section of the fiber and a schematic diagram of the network concept are shown Fig. 1. The SDM/WDM data layer is supported by a seed layer where the nodes can split, amplify, switch, and regenerate the seed signal to generate OFCs that share frequency-matched coherent transmission carriers and LOs across the network. Each node allows hybrid SDM/WDM add-drop multiplexing and supports the S, C, and L bands, thanks to wideband OFCs spanning a bandwidth of 134 nm, i.e., 50% wider bandwidth

than previously demonstrated [10]. This allowed the generation of 650 carriers for 3-mode transmission, with a net data rate exceeding 330 Tb/s per few-mode core and a potential for more than 12.7 Pb/s per fiber. Compared to Ref [11], we include more details on the frequency offset (FO) statistics of the received WDM channels when using synchronized transceiver combs. We measured 3 orders of magnitude lower frequency offset variations than conventional intradyne detection schemes, showing potential for simplifying the few-mode DSP. Moreover, in a single-mode transmission scenario, we demonstrate preliminary results about the possibility to share the DSP resources among the received channels thanks to the phase coherence of the comb carriers. We applied the phase noise estimated from a measured channel to neighbor channels, resulting in negligible performance penalty and showing the potential of wideband OFCs to enable lower DSP complexity and reduced power consumption through shared DSP schemes.

In this work, we report the widest comb used in a transmission experiment, as well as the widest regenerated comb from a transmitted seed signal. We also report the first few-mode transmission demonstration based on a comb source, achieving the highest data rate per fiber for a comb experiment in three spatial modes. The results show the potential of OFCs to enable cost-effective FM-MCF networks suitable for high-capacity datacenter interconnects.

II. SYSTEM DESCRIPTION

A. Parametric OFC Structure and Network Node

Figure 2(a) shows the structure of the OFC used in this work, which was developed by RAM Photonics [12]–[14]. The reader is referred to Refs. [12]–[14] for a thorough description of the comb design, as a detailed explanation is outside the scope of this work; in this section, we provide a simplified description. A stable RF oscillator drives a phase modulator to generate two 25 GHz-spaced carriers on a seed lightwave, which are amplified and then filtered with an etalon filter before entering a mixing stage. The etalon filter allows to remove excess amplified spontaneous emission (ASE) noise outside the carrier wavelengths for near-ideal seeding of the mixing stage. The latter is implemented using a dispersion-flattened highly nonlinear fiber to generate comb lines across a wide spectral band covering the S/C/L-bands [13]. The combs can be operated in master or slave configurations, where the seed lightwave is either a free-running laser with < 1 kHz linewidth (master), or a laser that is injection-locked to a reference seed (slave) [15].

When the comb is regenerated from a reference seed, the state of polarization (SOP) of the seed signal, which varies arbitrarily during transmission, needs to be aligned to the one required by the receiver comb. To achieve this, we used a lithium-niobate-based polarization synthesizer (Keysight N7786C) operating up to a rate of 40 kHz to track and set the SOP to the required one. The required SOP was predetermined maximizing the output power of an aligned polarizer; then, the synthesizer was capable of setting and maintaining the predetermined SOP, regardless of the input one.

The comb structure can be used to implement the network node shown in Fig. 2(b), which allows hybrid SDM/WDM

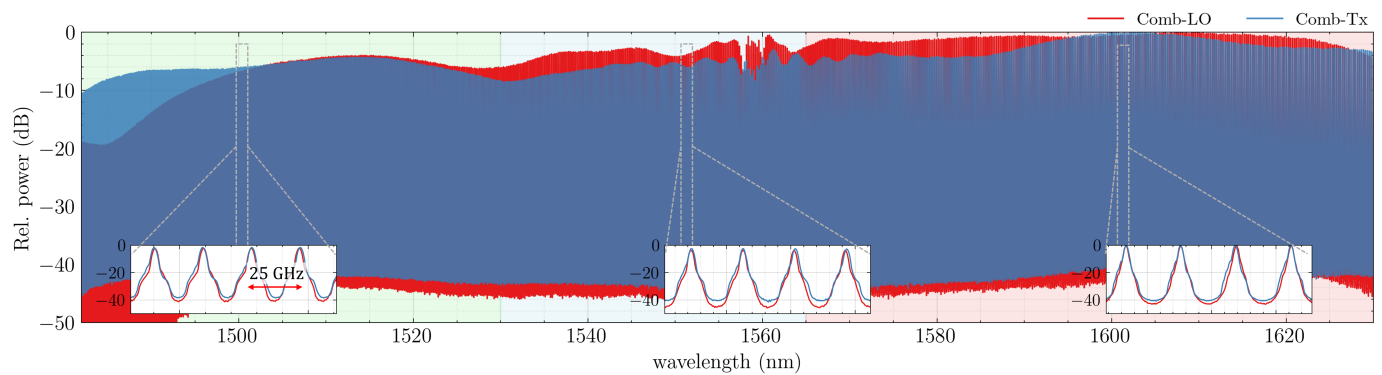


Fig. 3. Spectra of transmitter comb (Comb-Tx) and regenerated comb (Comb-LO) after seed transmission in the single-mode core #39 of 13-km-long FM-MCF. The shaded area in the figure background shows the boundaries between S/C/L bands.

add-drop functionality. It is assumed that all the OFCs in the network have access to a shared 10 MHz signal used as a reference by the RF oscillators, delivered, for example, by GPS systems [16]. By synchronizing the RF oscillators to the same 10 MHz clock signal, the lines of the different comb units maintain consistent spacing, preventing small frequency drifts that could occur with independent oscillators, which would introduce time-varying frequency offsets.

Figure 3 shows the transmitter and regenerated comb spectra after seed transmission, measured at a resolution of 0.02 nm. The spectra have < 4 dB power variations in the wavelength range 1500 nm to 1620 nm, excluding the variations around the seed wavelength of 1558.9 nm. The insets show a close-up view of the 25 GHz-spaced comb lines; the optical signal-to-noise ratio (OSNR) of the lines at 0.02 nm resolution exceeded 35 dB across all the bands.

B. Experimental Setup

The experimental setup implemented for demonstrating comb transmission and regeneration over FM-MCF is shown in Fig. 4. The transmitter comb output was split into two paths, one for generating a high quality sliding test-band, the other path for generating spectral dummy channels.

The sliding test-band was generated from three neighboring comb lines selected with a polarization maintaining (PM) tunable optical band-pass filter. The lines were separated into odd and even channels by interleavers (INT) before being modulated by a dual-polarization (DP)-IQ modulator driven by four 2-channel arbitrary waveform generators (AWGs) operating at 49 GS/s. The AWGs generated 24.5 GBaud polarization division multiplexed (PDM)-16QAM signals shaped with a root-raised cosine filter with a roll-off factor of 0.01 and with a length of 2^{16} symbols. The odd and even channels were decorrelated by inserting an optical delay of 150 ns.

Dummy WDM channels for the S, C, and L-bands were generated from the remainder of the comb carriers using a single polarization IQ (SP-IQ) modulator driven by electrically decorrelated outputs of a single AWG (see panel about dummy WDM generation in Fig. 4). To emulate polarization multiplexing, the SP-IQ output was split into two paths, and recombined using a polarization beam combiner (PBC) after adding a delay

of 100 symbols in one path. To produce a flat dummy channel spectrum in each of the transmission band, we used band-specific arbitrary programmable spectral filters, which we refer to as optical processors (OPs), implemented using wavelength-selective switch technology. The OPs were also used to carve a notch to accommodate the sliding test-band. Throughout the experimental setup we used WDM couplers to split and combine signals in each band, and Thulium (T) or Erbium (E) doped fiber amplifiers (DFAs) to compensate for the losses.

The combined WDM signal was then equally split. One path was used to generate the 3-mode test signal: this path was further divided by a 1×3 power splitter, with the output of each arm decorrelated using 100 m patch cords to emulate independent spatial signals for each mode. The second path was used to generate dummy SDM channels that were launched in the fiber cores adjacent to the cores carrying both data and seed, as detailed below. The transmission link consisted of a 13-km-long 39-core fiber with a cladding diameter of 312 μm , with the structure shown in Fig. 5. The fiber had 38×3 few-mode cores and a single-mode core (#39) used to transmit the seed lightwave for OFC regeneration without being affected by mode coupling. The single-mode core was originally included for direct comb seeding [6](in contrast to regenerated comb seeding performed in this work).

The cores were arranged in 3 concentric rings, and had a trench-assisted graded-index profile, except for the single-mode core #39, which had a step-index profile. The minimum inter-core distance was about 40 μm . Spatial multiplexing of the 114 spatial channels was achieved in two stages. First, the dummy and test SDM channel were connected to a high-port count optical switch (384×384); the latter assigned groups of three single-mode signals to the single-mode inputs of 38 non-mode-selective photonics lanterns (PLs) based on 3D waveguide technology. Next, the few-mode outputs of the PLs were spliced to the few-mode inputs of a free-space device, which coupled the 38 few-mode signals to the cores of the FM-MCF. Spatial de-multiplexing was achieved with the reverse process compared to the one described above. More details on the fiber specifications and on the multiplexers can be found in Ref. [17].

In our demonstration, we selected core #18 as the test core, which was located close to the single-mode core #39, and

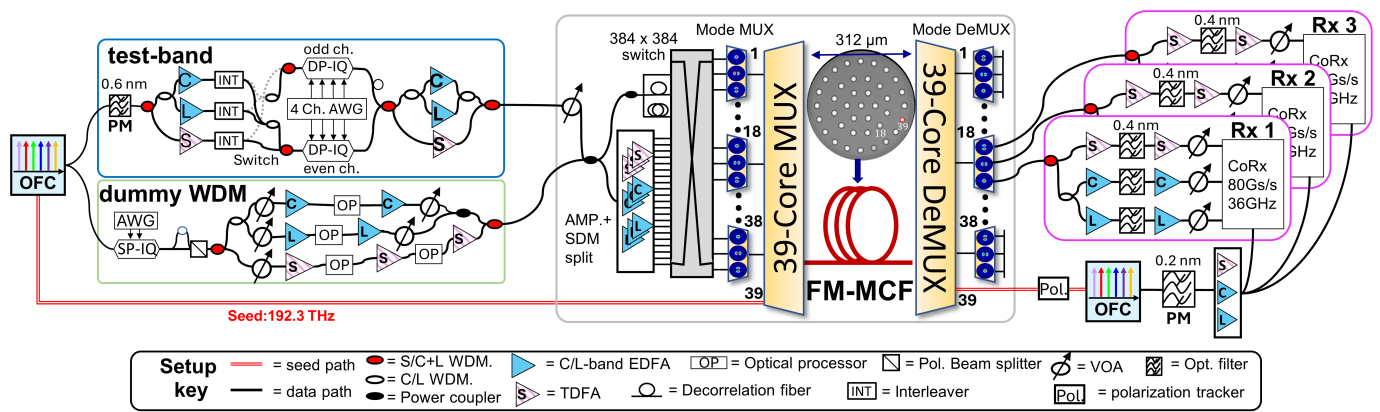


Fig. 4. Experimental setup for demonstration of SDM-WDM transmission with regenerated receiver comb in FM-MCF link with single-mode core channel (#39).

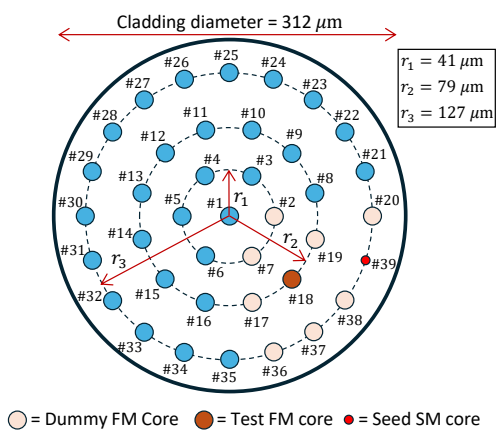


Fig. 5. Structure and core labelling for the high spatial density SDM fiber used in this work (previously presented in Ref. [17]). The fiber has 38×3 few-mode cores for data transmission, and an additional single-mode core (#39) for pilot tone transmission. For the experiments in this work, core #18 is the test core, and core #39 is used for comb seed transmission. The figure shows the dummy cores (loaded with 3-mode SCL-band dummy channels) selected adjacent to both core #18 and #39.

loaded only 8 adjacent cores with dummy channels (see Fig. 5) due to the limited availability of TDFAs in our laboratory. This is expected to not impact data-rate measurements as previous analyses on the same fiber [17], [18], showed that the cross-talk with non-neighbour cores is less than -50 dB, compared to the less than -40 dB cross-talk with the neighboring cores used in the experiment. Reference [17] also showed little wavelength dependence of the inter-core cross talk, suggesting that it mainly arose in the core multiplexing stage rather than during transmission. The power at the multiplexer input was set to 19 dBm per mode, and the span loss including the multiplexer was under 10 dB. The power of the seed signal at the output of the transmitter comb was 6 dBm.

At the receiver, the seed signal was fed to the active polarization tracking scheme described in Section II-A before being passed to the seed regeneration stage, which used an injection locked slave lasers. The regenerated seed was then input to another OFC for use as LO. The seed input power was about -9 dBm, which in our experiment was sufficient to achieve

injection locking within a 10 GHz locking bandwidth [15]. Long-term locking was achieved using a feedback control to manage drifts in the slave or master lasers bias currents or temperatures. For higher span losses than those considered in this work, the seed signal can be kept to a similar power level as the one in this experiment using optical amplification, as demonstrated in Ref. [10].

In the data path, after de-multiplexing the modes of core #18, the three single-mode signals were amplified, filtered by a 0.4-nm-wide tunable bandpass filter centered on the WDM channel under test, and amplified again. Optical patch cords were used to align the difference in path lengths to within a few centimeters to avoid excessive equalizer length at the receiver. We detected the signals with three synchronized coherent receivers (CoRx) that used the appropriate carrier of the regenerated comb, used to provide the LO carriers, selected using a 0.2-nm-wide tunable PM optical filter. To compensate for the losses on the LO path due to optical filtering and 1×3 splitting, we used band-specific PM optical amplifiers. The detected photocurrent signals were digitized at a sampling rate of 80 GS/s, and DSP was carried out offline. The latter consisted mainly of frequency offset estimation followed by few-mode least-mean squares MIMO equalization with 249 taps. The MIMO equalizer was first initialized in data-aided mode, switched to decision-directed after convergence; carrier phase-recovery was performed within the equalizer loop. The throughput of each channel was estimated from the generalized mutual information (GMI) and separately assessed using low-density parity-check (LDPC) codes from the DVB-S2 standard with code puncturing to achieve a code-rate granularity of 0.01. The highest code-rate resulting in a bit-error ratio (BER) below 5×10^{-5} was selected. The decoded data rate also included a 1% overhead due to a hard-decision outer forward error correction (FEC) code to eliminate remaining bit errors [19]. The performance was accessed over three 10 μs-long traces for each wavelength channel in turn.

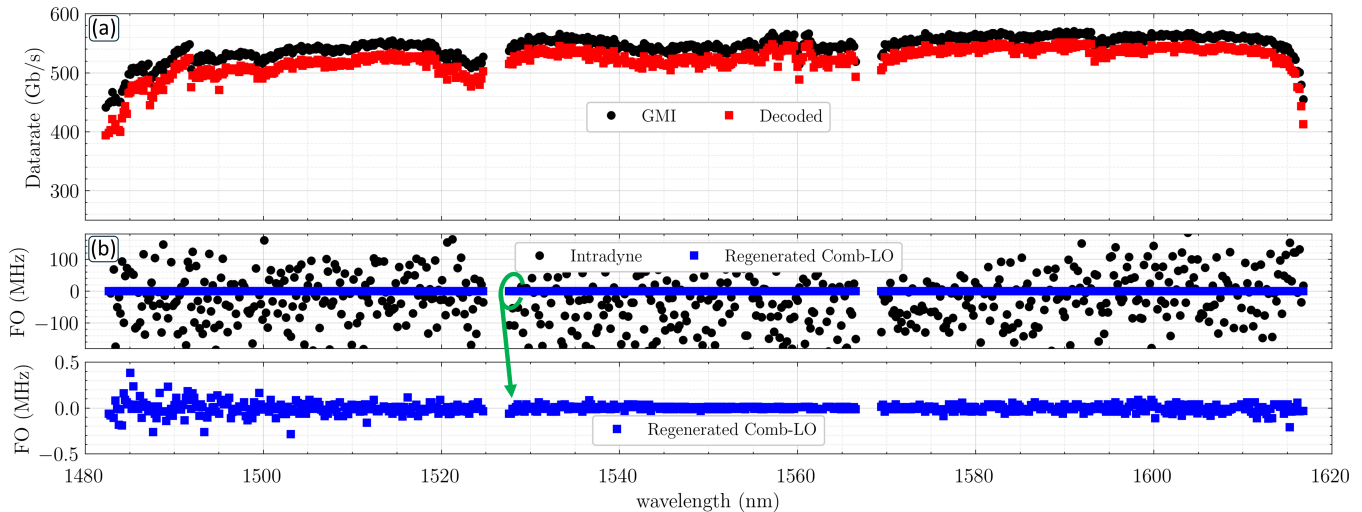


Fig. 6. (a) Data rate of the received 3-mode channels across S/C/L-band after transmission in FM core #18 and comb seed transmission on core #39. (b) Applied frequency offset (FO) corrections for regenerated comb as LO and comparison with intradyne configuration using an ECL as LO. The bottom part of the figure shows a close-up view of the FO when using synchronized transceiver combs.

III. RESULTS AND DISCUSSION

A. Transmission Results

Figure 6(a) shows the decoded and GMI estimated data rate of the 3-mode signals generated from the carriers of the transmitter comb, and received using a second comb regenerated from the transmitted seed as LO. The data rate is similar in the three bands, ranging from 500 to 560 Gb/s outside the bands extremes. Some data rate variations were observed in the C-band around the comb seed wavelength of 1558.9 nm due to a local reduced flatness of the comb [see Fig. 3]. Similarly, the lower S-band channels showed some variations in performance due to limited power in the LO comb. It was observed that fluctuations in operating temperature and small drifts in the seed wavelength caused variation in power for these channels. This behavior was consistent for both the transmitter and receiver combs; therefore, it is attributed to the response of the highly-nonlinear fiber used for comb broadening, rather than to the comb regeneration process. The best performance was obtained in the L-band where the combs had the highest carrier power and OSNR. The results showed no impact of incorrectly set SOP on the regenerated comb, suggesting that the update rate of the implemented polarization tracking was sufficient to track the polarization fluctuations occurring in the transmission fiber.

The total decoded data rate for the core under test was 336.3 Tb/s, achieved by 3-mode transmission of 650×24.5 GBaud PDM-16QAM signals, spanning a total bandwidth of 134 nm. These results suggest that a potential capacity of more than 12.7 Pb/s can be achieved per line side in network context. In our demonstration, the use of higher-order modulation formats was hindered by the presence of high-frequency phase noise in the comb carriers. This is attributed to the challenging design of the wideband and power-flat comb used in this study, particularly to phase noise accumulation in the four-wave mixing comb generation process, as detailed in [5], [20], [21], and also to the electronic circuitry within

the unit. This issue was not observed in our previous work that used C+L-band combs with a similar structure [10], suggesting that it is not an inherent feature and can be solved in subsequent comb development.

We report in Fig. 6(b) the FO correction applied to the received channels in the frequency recovery block when performing the DSP of the experimental data. We compared the performance obtained using synchronized transceiver combs with the one obtained by replacing the comb LO with a 10 kHz-linewidth tunable external cavity laser (ECL). Intradyne detection showed more than 100 MHz variations in FO across the bands, due to the incoherency between the transmitter and LO carriers. Alternatively, using the synchronized combs, the FO variations dropped by 3 orders of magnitude, indicating good alignment between the comb lines. The bottom part of Fig. 6(b) shows a close-up view of the FO values; the C-band channels had the best FO performance, as they are closer to the comb seed wavelength.

Although this work focused on comb regeneration after single-span transmission, to meet the requirements of the network structure shown in Fig. 1, the seed would need to be transmitted across multiple spans. This system would eventually face limitations on the number of amplifications and regenerations the seed can undergo due to noise accumulation, which would degrade the regenerated comb quality. While a thorough future analysis is needed to determine the performance degradation as a function of multiple amplification/regeneration stages, the feasibility of this approach has been demonstrated in Ref. [10].

B. Frequency Offset Analysis

To provide a more detailed analysis on the FO of the received channels, we simplified the system by switching to back-to-back (B2B) transmission. Basically, the new configuration is as shown in Fig. 4, but without the fiber link. The comb LO was regenerated after transmitting the seed from

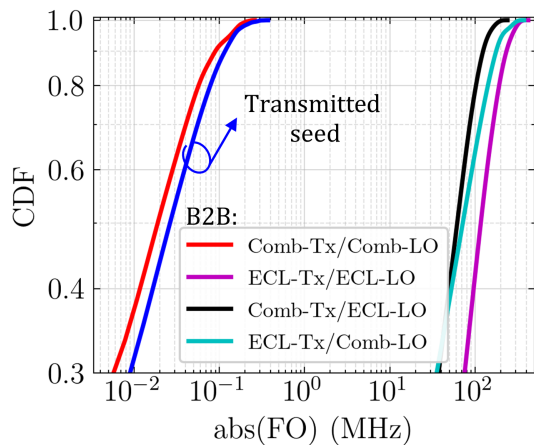


Fig. 7. CDF of the absolute value of the frequency offset of the received channels for the different transceivers configurations shown in the legend. Comb-Tx/Comb-LO denotes the transceiver configuration using comb carriers at the transmitter and synchronized comb carriers as LO. The other items in the legend follow analogous notation.

the master to the slave comb using PM patch cords. We investigated the FO across different transceiver configurations by replacing either the transmitter or LO comb lines with 10 kHz-linewidth ECLs. The analysis was performed on an ensemble of 260 measurements, composed of 52 channels (each acquired 5 different times with the oscilloscope) distributed across the bands. The results are shown in Fig. 7, where we plot the cumulative distribution functions (CDF) of the absolute value of the FO; the CDFs were obtained with kernel-based density estimation [22]. In accordance with what is presented in Section III-A, the configuration using synchronized combs (Comb-Tx/Comb-LO in the figure) achieved 3 orders of magnitude lower FO values compared to the intradyne configurations, with 99% probability of having the FO falling below 160 kHz. In the figure, we also compare the CDF obtained with the seed transmitted over the single-mode MCF core. It can be seen that the CDFs follow a similar statistic, indicating a good alignment between the comb lines even after seed transmission. The slight increase in FO is attributed to the ambient noise captured through the fiber.

C. Preliminary Analysis of Phase Coherence-Aided DSP

OFCs provide carriers that are phase-locked to a reference seed lightwave, meaning that the carriers have phase noise with correlated features. This property has become increasingly valuable for a variety of applications [23]. It has been shown that the phase information of neighboring WDM channels can be shared through shared DSP schemes [4], enabling lower DSP complexity and savings in power consumption. Yet, this approach has been so far demonstrated using comb structures that provide carriers over moderate bandwidths of less than 11 nm. Moreover, in previous works [4], extra DSP was required to account for the frequency offset among the transceiver carriers, as the receiver combs were not synchronized with the transmitter ones.

To validate the feasibility of shared DSP among the received channels, we conducted a single-mode, two-wavelength chan-

nel transmission experiment with 24.5GBaud PDM-16QAM signals, using the experimental setup shown in Fig. 8. Two C-band carriers of the transmitter comb at a distance of 1 nm were selected by two different 0.2 nm wide optical filters. The carriers had wavelengths of 1548.91 nm and 1549.91 nm, denoted in what follows as Channel 1 and Channel 2, respectively. The carrier lightwaves were modulated with two decorrelated sequences while maintaining the optical path alignment to within a few centimeters to preserve the phase noise correlation. To achieve decorrelated modulation (necessary for fair evaluation of shared phase recovery), a 100-symbol delay was applied to the Ch1 path before modulation using a fiber delay line, and the same delay was compensated in the Ch2 path before detection (see the decorrelation fiber in Fig. 8). This configuration allowed the use of a single IQ modulator for decorrelated modulation while preserving phase noise correlation.

After B2B transmission, the channels were detected with two synchronized coherent receivers, with LOs being filtered, path length aligned carriers from a regenerated receiver comb. We investigated the performance of the channels as a function of the OSNR by introducing an ASE noise loading stage before detection.

The DSP chain used a similar scheme to Ref. [4], and is shown in Fig. 9. For both channels, the processing blocks consisted of resampling at 2 Sa/sym, orthonormalization, matched filtering, timing recovery with the Lee algorithm [24]. Next, adaptive equalization was performed with 33 taps. The equalizer taps were first pre-converged with a constant modulus algorithm (CMA) for polarization demultiplexing [25]. After convergence, the taps were used to initialize a decision-directed (DD) least mean squares MIMO equalizer, with phase estimation contained in the equalizer loop. The latter was

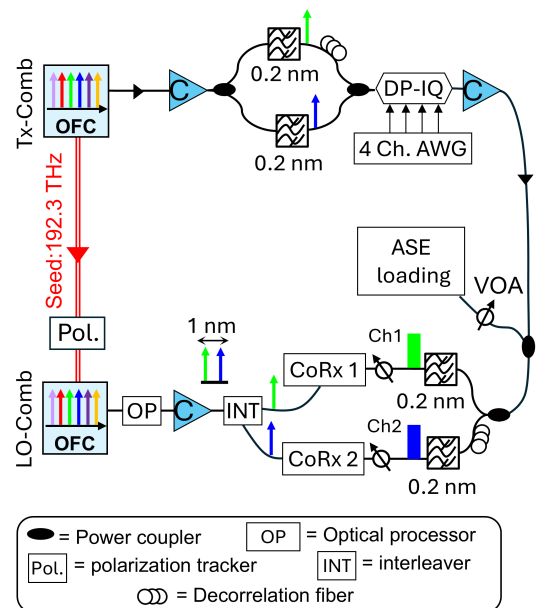


Fig. 8. Experimental setup for validation of shared DSP among two C-band channels (24.5 GBaud PDM-16QAM signals) separated by 1 nm after B2B transmission with noise loading stage.

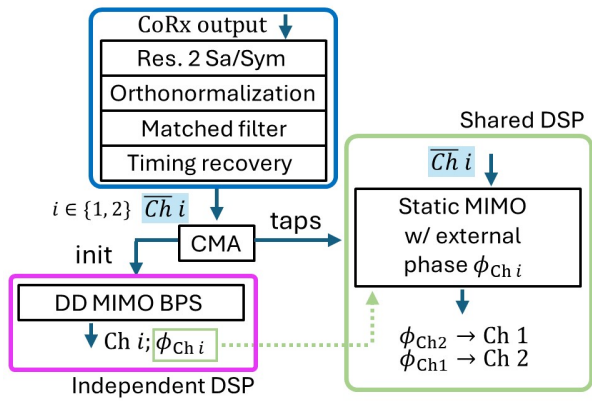


Fig. 9. Implemented DSP chain to compare the performance of independent versus shared DSP of two received channels in a single-mode PDM-16QAM 24.5 GBaud transmission experiment with transmitter comb source and regenerated comb as LO. Two channels at different wavelengths are first processed independently with a DD MIMO equalizer with BPS algorithm in the equalizer loop. Then, the phase estimate obtained from independent processing is shared among the channels.

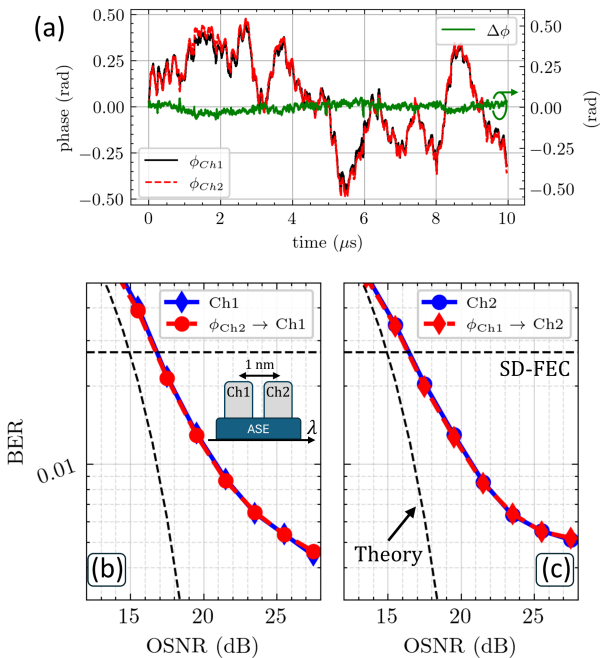


Fig. 10. Shared DSP for phase recovery of two received C-band channels with a wavelength separation of 1 nm in a single-mode 24.5 GBaud PDM-16QAM transmission experiment. (a) Phase estimated by the phase recovery block for the two channels; $\Delta\phi$ denotes the difference of the two phases. (b) BER versus OSNR for Ch1 processed independently (diamond markers) and Ch1 processed with phase estimated from Ch2 (circles); (c) BER performance as in (b) but with Ch1 and Ch2 switched in role. The vertical dashed black line shows the analytic expression for the BER of a 24.5 GBaud PDM-16QAM modulated system impaired by additive white Gaussian noise, whereas the horizontal black dashed line shows the 20% SD-FEC threshold at a BER of 2.7×10^{-2} .

implemented using the blind phase search (BPS) algorithm with 32 test phases and with an averaging block length of 512 symbols [26]. Initially, phase estimation and compensation were performed independently for Channel 1 and Channel 2 with the adaptive MIMO equalizer. Then, the phase estimate derived from Channel 1 was applied to compensate Channel 2,

and vice versa. This was done using a static MIMO equalizer that used the taps at the output of the CMA algorithm, with the use of the derived phase (see shared DSP block in Fig. 9).

The results are shown in Fig. 10(a)-(c). Figure 10(a) shows the phase noise resulting from the phase recovery block for the two channels, denoted as ϕ_{Ch1} and ϕ_{Ch2} , respectively. Highly correlated features can be observed, with a root-mean square of the phase difference, $\Delta\phi$, of about 1.3 degrees. Figures 10(b) and (c) compare the BER versus OSNR performance obtained by performing independent DSP of the channels (blue curves), to the one obtained from shared DSP (red curves). Negligible performance penalty was observed when sharing the estimated phase among the channels.

While this preliminary analysis considers two channels separated by 1 nm, the results demonstrate the potential of OFCs to simplify DSP complexity by requiring phase estimation for only a subset of the received channels. However, it is important to note that this analysis is limited to a small portion of the comb, and further investigations are needed to explore the performance of shared DSP over a wider bandwidth and in full multi-channel transmission scenario.

Further considerations regarding the associated challenges are discussed in what follows. As investigated in Ref. [27], the performance of shared carrier phase recovery degrades as the wavelength separation between channels increases. This degradation is caused by both line-dependent phase noise [4], and chromatic dispersion, which lead to phase noise decorrelation between channels. To mitigate this degradation, a potential strategy would be to employ multiple reference channels spaced across the WDM spectrum. For example, the reference channels could be spaced at intervals of 5 nm, sharing phase information with neighboring channels within ± 5 nm. By tuning the wavelength spacing, this approach enables a trade-off between minimizing performance penalties and achieving reduced complexity thanks to shared DSP.

Note also that while the demonstration in this section considered shared DSP between WDM channels in a single-mode fiber, the same approach can be applied to WDM channels transmitted within a spatial channel of an SDM link. Differently, using the phase noise recovered from a WDM channel of one spatial channel to compensate for the phase noise of a different WDM channel of a different spatial channel would be more critical, because modal delay would have a greater impact on the mutual correlation between the noise affecting the two channels.

IV. CONCLUSION

We have demonstrated regeneration of 134 nm bandwidth parametric optical frequency combs in a large-scale few-mode multi-core fiber network link, with a single-mode channel for seed transmission. Such a link can provide ultra-high capacity interconnects in network architectures exploiting OFC and SDM technology. The results suggest that a potential throughput of 12.7 Pb/s per line side can be achieved with similar performance in all cores. These results show that in a seeded-comb optical network architecture, the combination of OFC and SDM technology may not only enable the saving hundreds

of transmitter and receiver lasers with a single device, but also reduce the digital signal processing complexity and provide savings in power consumption by leveraging phase-coherent and frequency-locked carriers.

V. ACKNOWLEDGMENTS

We thank Evgeny Myslivets for support on comb operation.

REFERENCES

- [1] B. J. Puttnam, R. S. Luís, W. Klaus, J. Sakaguchi, J.-M. Delgado Mendinueta, Y. Awaji, N. Wada, Y. Tamura, T. Hayashi, M. Hirano, and J. Marcianti, "2.15 Pb/s transmission using a 22 core homogeneous single-mode multi-core fiber and wideband optical comb," in *2015 European Conference on Optical Communication (ECOC)*, 2015, pp. 1–3.
- [2] Y. Awaji, J. Sakaguchi, B. J. Puttnam, R. S. Luís, J. M. D. Mendinueta, W. Klaus, and N. Wada, "High-capacity transmission over multi-core fibers," *Optical Fiber Technology*, vol. 35, pp. 100–107, Feb. 2017.
- [3] M. Mazur, J. Schröder, M. Karlsson, and P. A. Andrekson, "Joint Superchannel Digital Signal Processing for Effective Inter-Channel Interference Cancellation," *Journal of Lightwave Technology*, vol. 38, no. 20, pp. 5676–5684, 2020.
- [4] L. Lundberg, M. Mazur, A. Mirani, B. Foo, J. Schröder, V. Torres-Company, M. Karlsson, and P. A. Andrekson, "Phase-coherent lightwave communications with frequency combs," *Nat Commun*, vol. 11, no. 1, p. 201, Jan. 2020.
- [5] A. Lorences-Riesgo, T. A. Eriksson, A. Fulop, P. A. Andrekson, and M. Karlsson, "Frequency-Comb Regeneration for Self-Homodyne Superchannels," *J. Lightwave Technol.*, vol. 34, no. 8, pp. 1800–1806, Apr. 2016.
- [6] J. Sakaguchi, W. Klaus, B. J. Puttnam, J. M. D. Mendinueta, Y. Awaji, and N. Wada, "Spectrally-Efficient Seed-Lightwave-Distribution System using Space-Division-Multiplexed Distribution Channel for Multi-core 3-Mode-Multiplexed DP-64QAM Transmission," in *2017 European Conference on Optical Communication (ECOC)*, 2017, pp. 1–3.
- [7] M. Mazur, J. Schröder, A. Lorences-Riesgo, T. Yoshida, M. Karlsson, and P. A. Andrekson, "12 b/s/Hz Spectral Efficiency Over the C-band Based on Comb-Based Superchannels," *Journal of Lightwave Technology*, vol. 37, no. 2, pp. 411–417, 2019.
- [8] J. Sakaguchi, Y. Awaji, and H. Furukawa, "Ultra-long-distance distribution of low-phase-noise reference lightwave for optical communications," *Opt. Express*, vol. 31, no. 13, pp. 20 715–20 729, Jun 2023.
- [9] B. J. Puttnam, R. S. Luis, G. Rademacher, G. Di Sciullo, M. Van Den Hout, J. Sakaguchi, C. Antonelli, C. Okonkwo, and H. Furukawa, "C + L-band seeded comb regeneration for MCF networks," in *49th European Conference on Optical Communications (ECOC 2023)*. Hybrid Conference, Glasgow, UK: Institution of Engineering and Technology, 2023, pp. 393–396.
- [10] B. J. Puttnam, R. S. Luis, D. Orsuti, G. Rademacher, G. D. Sciullo, M. van den Hout, J. Sakaguchi, C. Antonelli, C. Okonkwo, L. Palmieri, and H. Furukawa, "Experimental demonstration of a multi-core fiber seeded comb optical network (MCF-SCON)," *J. Opt. Commun. Netw.*, vol. 16, no. 7, pp. C69–C75, Jul 2024.
- [11] B. J. Puttnam, D. Orsuti, R. S. Luis, M. S. Neves, J. Sakaguchi, C. Antonelli, C. Okonkwo, L. Palmieri, and H. Furukawa, "Wideband S, C,+ L-Band Comb Regeneration in Large-Scale Few-Mode MCF Link with Single-Mode Seed Channel," in *Optical Fiber Communication Conference*, San Diego, California, 2024, p. Th4A.6.
- [12] B. P.-P. Kuo, E. Myslivets, V. Ataie, E. G. Temprana, N. Alic, and S. Radic, "Wideband Parametric Frequency Comb as Coherent Optical Carrier," *Journal of Lightwave Technology*, vol. 31, no. 21, pp. 3414–3419, 2013.
- [13] V. Ataie, E. Myslivets, B. P.-P. Kuo, N. Alic, and S. Radic, "Spectrally Equalized Frequency Comb Generation in Multistage Parametric Mixer With Nonlinear Pulse Shaping," *Journal of Lightwave Technology*, vol. 32, no. 4, pp. 840–846, 2014.
- [14] V. Ataie, E. Temprana, L. Liu, E. Myslivets, B. P.-P. Kuo, N. Alic, and S. Radic, "Ultrahigh Count Coherent WDM Channels Transmission Using Optical Parametric Comb-Based Frequency Synthesizer," *Journal of Lightwave Technology*, vol. 33, no. 3, pp. 694–699, 2015.
- [15] Z. Liu and R. Slavík, "Optical Injection Locking: From Principle to Applications," *Journal of Lightwave Technology*, vol. 38, no. 1, pp. 43–59, 2020.
- [16] M. Lombardi, "The Use of GPS Disciplined Oscillators as Primary Frequency Standards for Calibration and Metrology Laboratories," *Measurement: The Journal of Measurement Science*, no. 3, 2008-09-01 2008.
- [17] J. Sakaguchi, W. Klaus, Y. Awaji, N. Wada, T. Hayashi, T. Nagashima, T. Nakanishi, T. Taru, T. Takahata, and T. Kobayashi, "228-Spatial-Channel Bi-Directional Data Communication System Enabled by 39-Core 3-Mode Fiber," *Journal of Lightwave Technology*, vol. 37, no. 8, pp. 1756–1763, 2019.
- [18] B. J. Puttnam, M. van den Hout, G. Di Sciullo, R. S. Luis, G. Rademacher, J. Sakaguchi, C. Antonelli, C. Okonkwo, and H. Furukawa, "22.9 Pb/s Data-Rate by Extreme Space-Wavelength Multiplexing," in *49th European Conference on Optical Communications (ECOC 2023)*, vol. 2023, 2023, pp. 1678–1681.
- [19] G. Rademacher, R. S. Luis, B. J. Puttnam, T. A. Eriksson, R. Ryf, E. Agrell, R. Maruyama, K. Aikawa, Y. Awaji, H. Furukawa, and N. Wada, "High Capacity Transmission With Few-Mode Fibers," *J. Lightwave Technol.*, vol. 37, no. 2, pp. 425–432, Jan. 2019.
- [20] J. C. Skehan, C. Naveau, J. Schroder, and P. Andrekson, "Widely tunable, low linewidth, and high power laser source using an electro-optic comb and injection-locked slave laser array," *Opt. Express*, vol. 29, no. 11, pp. 17 077–17 086, May 2021.
- [21] J. C. Skehan, Óskar B. Helgason, J. Schröder, V. Torres-Company, and P. A. Andrekson, "Widely tunable narrow linewidth laser source based on photonic molecule microcombs and optical injection locking," *Opt. Express*, vol. 30, no. 13, pp. 22 388–22 395, Jun 2022.
- [22] B. W. Silverman, *Density Estimation for Statistics and Data Analysis*, 1st ed. Routledge, 1998.
- [23] T. Fortier and E. Baumann, "20 years of developments in optical frequency comb technology and applications," *Commun Phys*, vol. 2, no. 1, p. 153, Dec. 2019.
- [24] D. Lee and K. Cheun, "A new symbol timing recovery algorithm for OFDM systems," *IEEE Transactions on Consumer Electronics*, vol. 43, no. 3, pp. 767–775, 1997.
- [25] F. P. Guiomar, S. B. Amado, A. Carena, G. Bosco, A. Nespola, A. L. Teixeira, and A. N. Pinto, "Fully Blind Linear and Nonlinear Equalization for 100G PM-64QAM Optical Systems," *Journal of Lightwave Technology*, vol. 33, no. 7, pp. 1265–1274, 2015.
- [26] H. Sun, K.-T. Wu, S. Thomson, and Y. Wu, "Novel 16QAM carrier recovery based on blind phase search," in *2014 The European Conference on Optical Communication (ECOC)*, 2014, pp. 1–3.
- [27] L. Lundberg, M. Karlsson, A. Lorences-Riesgo, M. Mazur, V. Torres-Company, J. Schröder, and P. Andrekson, "Frequency Comb-Based WDM Transmission Systems Enabling Joint Signal Processing," *Applied Sciences*, vol. 8, no. 5, p. 718, May 2018.